무한요소를 이용한 지반-구조물 상호작용해석 :
강제진동 및 지진응답 해석
Soil-Structure Interaction Analysis by Infinite Elements :
Simulation of Forced Vibration and Earthquake Responses

윤 정 방*   양 신 추**   김 재 민***
Yun, Chung Bang   Yang, Shin Chu   Kim, Jae Min

요   약

동적무한요소를 이용한 지반-구조물 상호작용에 대하여 연구하였다. 동적무한요소는 무한원 방향으로 전파되어 나가는 여러종류의 지진파 성분을 동시에 모형화 할 수 있도록 개발된 축대칭요소로서, 구조물에서 멀리 떨어진 지반영역(외부영역)을 모형화 하는데 사용되었다. 반면, 구조물에 가까운 지반영역(내부영역)은 재래의 축대칭요소를 사용하여 모형화 하였다. 본 해석방법의 검증은 적층된 반무한 지반위에 놓여진 원형강판의 임피던스함수를 구하여, 이를 이론적 결과와 비교하는 방법으로 수행되었다. 또한, 지반에 일부가 묻힌 원통형구조물에 대하여 수행된 강제진동시험 결과와 실제 지진발생시 구조물의 거동기록을 같은 입력조건에 대하여 본 해법으로 구한 결과와도 비교하였다. 해석결과로 부터 본 해석방법이 구조물의 거동을 타당히 산정하여 줌을 알 수 있었다.

1. INTRODUCTION

This paper presents a study on soil-structure interaction analysis using dynamic infinite elements. Axisymmetric dynamic infinite elements, which were developed for modelling the effect of propagating multi-wave components into the infinite directions by the present authors[1], are utilized for modelling the far field of the unbounded soil media. Verifications of the present analysis method using the infinite elements are carried out for a circular rigid plate on a layered half-space and also for an embedded cylindrical structure subjected to forced excitations. Analysis is also carried out to simulate the earthquake response of the cylindrical structure during an earthquake event. The results from the analyses indicate that the present method using the infinite elements predicts reasonable structural responses compared with the measured responses and the computed ones by using other computer code.

2. DYNAMIC INFINITE ELEMENTS INCLUDING NODELESS VARIABLES

In this study, the axisymmetric infinite elements, which were developed by the present authors[1], are utilized. They have three nodes placed on the interface between the near and the far fields as in *Figure 1*. However, it can include an arbitrary number of wave components in its shape functions by introducing nodeless variables. The concept of the nodeless variable is similar to the internal variables in the classical finite element, which are added to include shape functions having zero values at the nodes but nonzero values inside the element.

*   정회원, 한국과학기술원 토목공학과 교수
** 정회원, 한국고속철도건설공단 연구개발본부 선임연구원 (공학박사)
*** 한국과학기술원 토목공학과 박사과정

Geometrical Mapping

For analyzing a layered half-space consisting of horizontal layers and a half-space below the layers as shown in *Figure 1*, two kinds of the axisymmetric infinite elements were developed; i.e., horizontal and radiational infinite elements. The mapping of the infinite elements from the local coordinates (ξ, η) to the global coordinates (r, z) are defined as:

For horizontal infinite elements,

$$r = \sum_{j=1}^{3} M(\xi) L_j(\eta) r_j \quad , \quad z = \sum_{j=1}^{3} L_j(\eta) z_j \tag{1}$$

For radiational infinite elements,

$$r = \sum_{j=1}^{3} M(\xi) L_j(\eta) r_j \quad , \quad z = \sum_{j=1}^{3} M(\xi) L_j(\eta) z_j \tag{2}$$

where $L_j(\eta)$ is a Lagrange polynomial of which value at node j is unity, and $M(\xi)$ is the mapping function$(= 1 + \xi)$ for the infinite direction.

Displacement Shape Functions

A typical displacement component in the r-direction may be expressed as a linear combination of several wave components as

$$u(\mathbf{x}) = \sum_{l=1}^{N} \{\sum_{j=1}^{3} L_j(\eta) a_{lj}^u\} F_l^u(\mathbf{x}) \tag{3}$$

where $\mathbf{x} = \langle r, z \rangle^T$; a_{lj}^u is a generalized parameter associated with the l-th wave component and the j-th Lagrange polynomial; N is the number of wave components employed; $F_l^u(\mathbf{x})$ is the function representing the l-the wave component in the form of $e^{-(\alpha\xi + ik_l R)}$ or $e^{-(\alpha\xi + ik_l r)}$, which satisfies the Sommerfeld radiation condition. In the previous expression R denotes the radiational distance from the origin, and k_l is the wavenumber of the l-th wave component.

By utilizing the nodal displacement U_j and the generalized parameters for nodeless variables a_{lj}^u $(l \geq 2)$, Equation (3) can be rewritten as

$$u(x) = \sum_{j=1}^{3} L_j(\eta) \frac{F_1^u(\mathbf{x})}{F_1^u(\mathbf{x}_j)} U_j + \sum_{l=2}^{N} \sum_{j=1}^{3} L_j(\eta) \{F_l^u(\mathbf{x}) - \frac{F_l^u(\mathbf{x}_j)}{F_1^u(\mathbf{x}_j)} F_1^u(\mathbf{x})\} a_{lj}^u \tag{4}$$

From Equation (4), the shape functions for the nodal displacements are

$$N_j^u(\mathbf{x}) = L_j(\eta) \frac{F_1^u(\mathbf{x})}{F_1^u(\mathbf{x}_j)} \quad \text{for} \quad j = 1, 2, 3 \tag{5}$$

and those for the nodeless variables are

$$N_j^u(\mathbf{x}) = L_k(\eta) \{F_l^u(\mathbf{x}) - \frac{F_l^u(\mathbf{x}_j)}{F_1^u(\mathbf{x}_j)} F_1^u(\mathbf{x})\} \quad \begin{array}{l} \text{for} \quad j = 3(l-1) + k \\ (k = 1, 2, 3; \ l = 2, 3, \cdots, N) \end{array} \tag{6}$$

The displacements associated with the nodeless variables in Equation (6) are no longer restricted to be zero along the interfaces with the neighboring infinite elements. Hence, to preserve the displacement continuities along the interfaces, the nodeless variables for each wave component including nonzero displacements along the interface are taken to be equal to those of neighboring elements. The compatibility condition between the finite and the infinite elements can be also kept, if the wave function has a constant value on the interface as those for the horizontal infinite element.

The displacement shape function in the θ- and z-direction , $N_j^v(\mathbf{x})$ and $N_j^w(\mathbf{x})$, can be constructed similarly to the above procedure.

Numerical Integrations

For constructing the element stiffness and mass matrices of a dynamic infinite element, which includes multi-wave components, it is required to carry out integrations extending to infinity as

$$I = \int_0^\infty \{ \sum_{l=1}^N f_l(\xi) \, e^{-(\alpha_l + i\beta_l)\xi} \}^2 \, d\xi \tag{7}$$

For a computation efficiently, Equation (7) can be rewritten as

$$I = \sum_{l=1}^N \sum_{j=1}^N \int_0^\infty P_{ij}(\frac{\zeta}{\theta_{ij} + i\delta_{ij}}) e^{-\zeta} \frac{d\zeta}{\theta_{ij} + i\delta_{ij}} \tag{8}$$

Then, using the Gauss-Laguerre quadrature the integral can be evaluated as

$$I \cong \sum_{l=1}^N \sum_{j=1}^N \{ \sum_{k=1}^{M_{req}} P_{ij}(\tilde{\xi}_k) \, \tilde{W}_k \} \tag{9}$$

where M_{req} is the number of the integration points used, and $\tilde{\xi}_k$ and $\tilde{W}_k$ are the new integration point and the corresponding weighting factor[1,2].

3. EXAMPLE ANALYSIS AND DISCUSSIONS

Circular Footing on Elastic Half-Space

For the verification of the present analysis method, impedance functions of rigid circular plates on an elastic homogeneous half-space and on a layered half-space are computed for the horizontal and the rocking motions. The soil properties are shown in *Figure 1*. Wave functions employed for the formulation are shown in *Table 1*. The computed impedance functions for a layered half-space are compared with the analytical results[3] in *Figure 2*. The results indicate that the present analysis using infinite elements gives very good results.

Simulation of Forced Vibration Test

Verification of the present analysis procedure is carried out by using the forced vibration test data on an embedded cylindrical structure reported in Reference 4, As in *Figure 3*, horizontal excitation forces are applied at the top of the structure, and the horizontal velocity at the top is measured. Then the transfer function for the top displacement is evaluated. Numerical analysis is carried out using the model in *Figure 3*. Based on the soil test data, the shear wave velocity of the far field is approximately taken as 300 *m/sec*, while that of near field 210 *m/sec*. Other soil properties are taken to be same in the near and far fields: the damping ratio(ξ) =6 %, the mass

density $=1.8$ ton/m^3, and the poisson's ratio $=0.211$. In the linear analysis, the dynamic shear moduli of the soil media are taken to those corresponding to small strain. On the other hand, in the nonlinear analysis, those are assumed to be dependent on the strain. Comparison with the test data as shown in *Figure 4*, the linear analysis results are found to be fairly deviated from the measured one, while the nonlinear results agree fairly well. For the purpose of comparison, another linear analysis is carried out using the soil properties used in other study[4]. The shear wave velocity is taken to be 210 *m/sec* for the near and far field regions. As shown in *Figure 4*, the present analysis result is found to be very well compared with those in the study using a computer code HASSI-4, which is based on the hybrid soil-structure interaction analysis method[5].

Simulation of Earthquake Response

In this example, it is tried to simulate the response of a cylindrical structure (*Figure 5*) during an earthquake event with a relatively small amplitude. The structure is the one used in the forced vibration analysis. *Figures 6* and *7* show the time histories of the recorded horizontal ground accelerations at observation point S1 (*Figure 5*) and the structural responses at the top. The analysis model used in the forced vibration analysis as in *Figure 3* is also utilized in this example. In the equation of motion, the effective earthquake forces are expressed in terms of the free field motion at the interface between the structure and the soil medium[2]. The recorded ground motions at two observation points (S1 and A1 in *Figure 5*) near the structure are utilized as two different samples for the input free field motion.

Since the peak ground acceleration was about $0.005g$, the linear analysis is carried out by using the degraded soil properties: the shear wave velocity in the near and far field regions $=275$ *m/sec* and the damping ratio $=2\%$. Other properties are taken to be the same as those used in the forced vibration analysis. The computed responses using the recorded ground accelerations at S1 by the present method are compared with the recorded ones in *Figures 6* and *7*. The computed responses by a computer program HASSI-4 [4] are also shown in the figures. The results show that the NS component of the simulated responses by the present method are found to be in good agreement with the observed responses, while the EW component is consistently smaller than the observed ones. However, it is very interesting to notice that the results by the present method agree very well with those by HASSI-4 code. At the present moment, it is not quite clear why the analysis results for the EW components are poor, while those for the NS component are excellent. It might be caused by the different soil properties in two directions, particularly in the far field region. Further investigations are required to clarify the reasons.

REFERENCES

1. Yang, S-C. and Yun, C-B., "Axisymmetric infinite elements for soil-structure interaction analysis ," *Engineering Structures*, Vol.14, No.6, 1992, pp.361-370.
2. Yang, S-C., "Dynamic Infinite elements for soil-structure analysis," *Ph.D. Dissertation*, Korea Advanced Institute of Science and Technology, 1992.
3. Luco, J.E., "Impedance functions for a rigid foundation on a layered medium." *Nuclear Engineering and Designs*, Vol. 31, 1974, pp.204-217.
4. Katayama, I., Ohsumi, T., and Teramura, Y., "Experimental Validation of Soil-Structure Interaction Analysis," *Proc. of the US-Korea Joint Seminar on Critical Engineering System*, Vol.1, pp.496-506, Seoul Korea, 1987.
5. Gupta, S., Penzien, J., Lin, T.W., and Yeh, C.S., "Three-dimensional hybrid modelling of soil-structure interaction," *Earthquake Engineering and Structural Dynamics*, Vol.10, 1982, pp.69-87.

Table 1. Wave Functions $F(x)$'s for Homogeneous Half-Space and Layered Half-Space

Wave components	Rayleigh	Love	Shear	Compressional
Homogeneous Half-Space	$e^{-(\alpha\xi+ik_r r)}$	---	$e^{-(\alpha+ik_r R_0)\xi}$	$e^{-(\alpha+ik_p R_0)\xi}$
Horizontal Layer (Layered Half-Space)	$e^{-(\alpha+ik_r R_0)\xi}$	$e^{-(\alpha+ik_L R_0)\xi}$	---	---
Underlying Half-Space (Layered Half-Space)	---	---	$e^{-(\alpha+ik_s R_0)\xi}$	$e^{-(\alpha+ik_p R_0)\xi}$
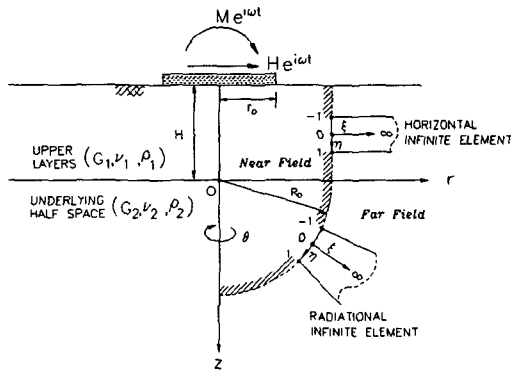
Example Case :

$$V_{S1} / V_{S2} = 0.8$$

$$\rho_1 / \rho_2 = 0.85$$

$$\nu_1 = \nu_2 = 0.25$$
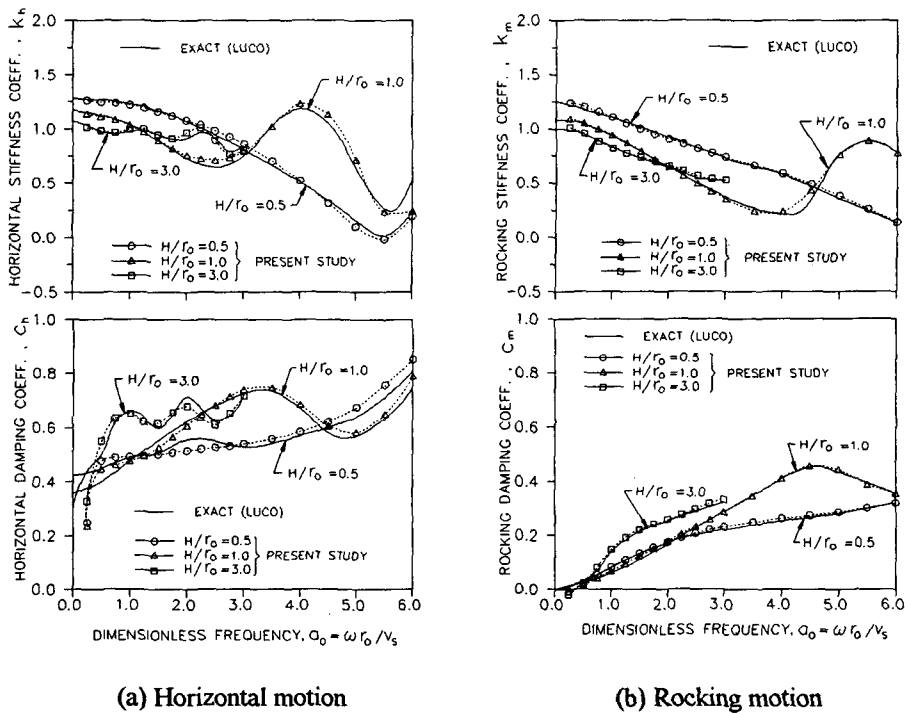
Figure 1. Circular footing on a layered half-space

(a) Horizontal motion

(b) Rocking motion

Figure 2. Impedance functions for a layered half-space ($\alpha = 0.75$, $R_0 / r_0 = 2.0$)

Figure 3

EXCITATION FORCE

2.0ᵐ

8.5ᵐ

BEAM ELEMENT

1.2ᵐ

1.5ᵐ

TOTAL WEIGHT OF STRUCTURE	98.0(ton)
WEIGHT OF VIBRATOR	2.5(ton)

4.5ᵐ

1.5ᵐ

∞ ∞ ∞ ∞ ∞ ∞ ∞ ∞ ∞

INFINITE ELEMENT

SOLID ELEMENT
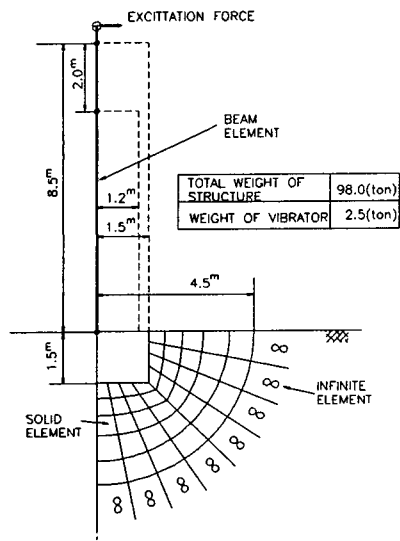
Figure 3. Analysis model for forced vibration test

Figure 4

$V_S^0 = 210 \text{m/s}$
$V_S^i = 210 \text{m/s}$
—— Linear
----- HASSI-4

$V_S^0 = 210 \text{m/s}$
$V_S^i = 300 \text{m/s}$
—— Linear
----- Nonlinear

● OBSERVED DATA

AMPLITUDE (mm/ton)
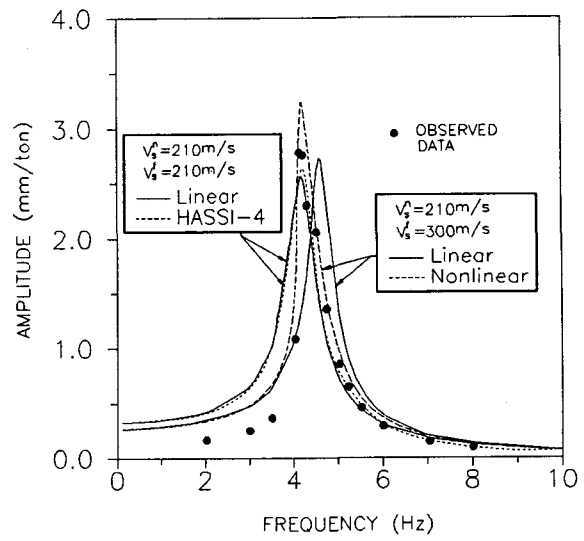
FREQUENCY (Hz)

Figure 4. Amplitude of the frequency response function for the top displacement

Figure 5

OBSERVATION POINT OF TOP ACCELERATION

N

A1

8.5m

1.5m

1.5m

S1

A2

200m

200m

200m

30m

A1

S1

STRUCTURE

1.5m
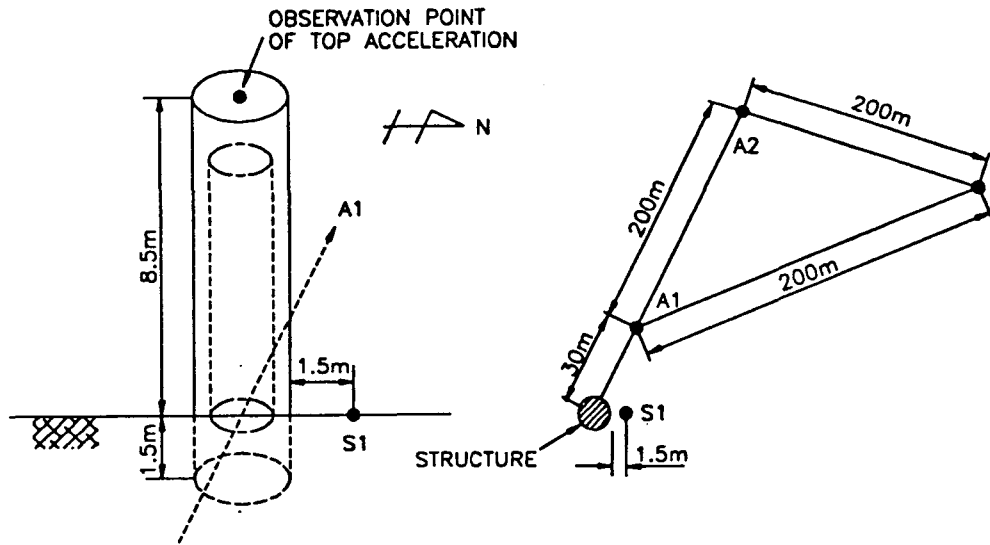
Figure 5. Observation points of seismic motions

(a) Observed ground acceleration at S1

(b) Observed response

(c) Calculated response by the present method

(d) Calculated response by HASSI-4

Figure 7. Observed ground motion (at S1) and structural response (at the top) and the calculated response (EW-Components)

(a) Observed ground acceleration at S1

(b) Observed response

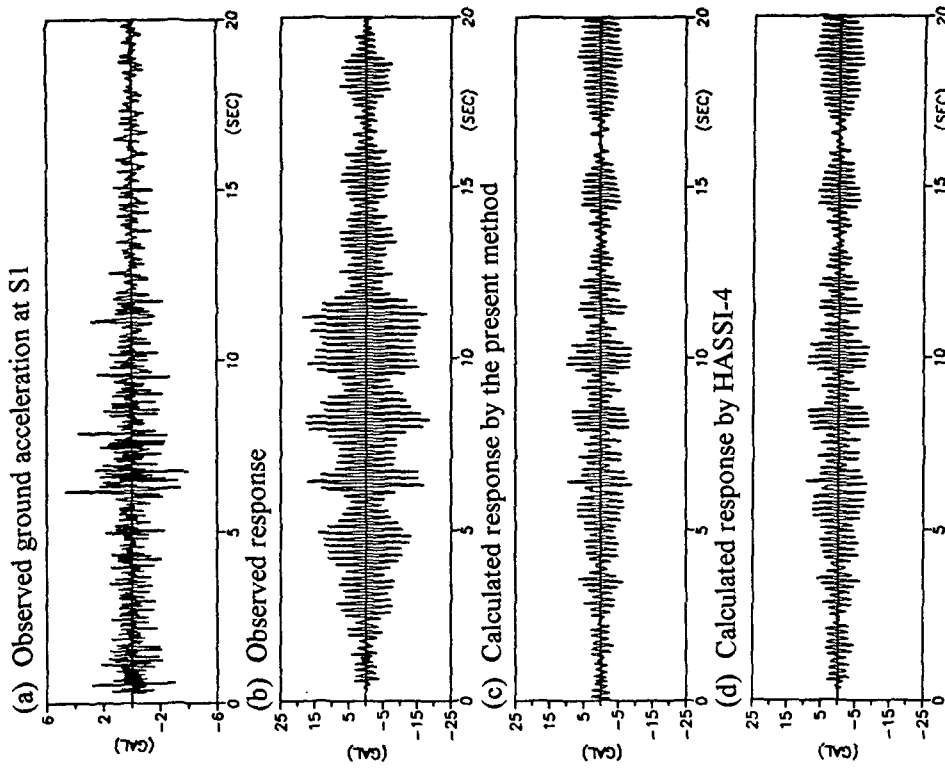(c) Calculated response by the present method

(d) Calculated response by HASSI-4

Figure 6. Observed ground motion (at S1) and structural response (at the top) and the calculated response (NS-Components)